



OPEN

# Structural origin of light emission in germanium quantum dots

SUBJECT AREAS:  
ELECTRONIC PROPERTIES  
AND MATERIALS  
NANOPARTICLESW. Little<sup>1</sup>, A. Karatutlu<sup>1,2</sup>, D. Bolmatov<sup>5</sup>, K. Trachenko<sup>1</sup>, A. V. Sapelkin<sup>1</sup>, G. Cibin<sup>3</sup>, R. Taylor<sup>3</sup>,  
F. Mosselmans<sup>3</sup>, A. J. Dent<sup>3</sup> & G. Mountjoy<sup>4</sup>Received  
4 June 2014Accepted  
3 November 2014Published  
9 December 2014Correspondence and  
requests for materials  
should be addressed to  
A.V.S. (a.sapelkin@  
qmul.ac.uk)

<sup>1</sup>Center for Condensed Matter and Materials Physics, School of Physics and Astronomy, Queen Mary, University of London, Mile End Road, London E1 4NS, UK, <sup>2</sup>Electrical and Electronics Engineering, Yildirim Campus, Bursa Orhangazi University, 16245, Yildirim, Bursa, Turkey, <sup>3</sup>Diamond Light Source Ltd, Didcot OX11 0DE, Oxon, UK, <sup>4</sup>School of Physical Sciences, University of Kent, Canterbury, CT2 7NZ, UK, <sup>5</sup>Baker Laboratory, Cornell University, Ithaca, New York 14853, United States.

We used a combination of optically-detected x-ray absorption spectroscopy with molecular dynamics simulations to explore the origins of light emission in small (5 nm to 9 nm) Ge nanoparticles. Two sets of nanoparticles were studied, with oxygen and hydrogen terminated surfaces. We show that optically-detected x-ray absorption spectroscopy shows sufficient sensitivity to reveal the different origins of light emission in these two sets of samples. We found that in oxygen terminated nanoparticles its the oxide-rich regions that are responsible for the light emission. In hydrogen terminated nanoparticles we established that structurally disordered Ge regions contribute to the luminescence. Using a combination of molecular dynamics simulations and optically-detected x-ray absorption spectroscopy we show that these disordered regions correspond to the disordered layer a few Å thick at the surface of the simulated nanoparticle.

It is well known that the reduction of size down to the nano-scale can have a significant impact on the physical properties of a material. For semiconductors this can generally be understood in terms of the quantum confinement effect - a condition where the geometric size decisively affects a variety of physical parameters<sup>1,2</sup>. The concept is elegant, but not easy to probe directly in many cases due to the difficulties in observing quantum dots (QDs) in an idealised state that can be readily compared with a corresponding theoretical or a computational model. A good example of this is porous nanocrystalline Si (*p*Si), the unusual optical properties of which were discovered in 1990 by Canham<sup>3</sup>. The intense visible photoluminescence (PL) observed in *p*Si was originally attributed to the quantum confinement effect, but almost immediately another point of view was voiced<sup>4,5</sup> suggesting the effect was due to the surface or silicon compounds of a molecular nature on the surface. Over two decades of intense research followed that could not provide unequivocal evidence and eventually led to the development of a model of Si QDs that includes a core, surface, and interfacial regions<sup>6</sup>. Contributions to the discussion include rather complex PL measurements on single Si QDs in a silicon oxide environment<sup>7</sup>, in magnetic fields<sup>8</sup> and under high pressure<sup>9</sup>. Crucially, none of the approaches so far have been able to provide *direct* evidence of a connection between the light emission and the underlying atomic structure. It seems that the research into Ge QDs is suffering from a similar fate. Several preparation routes have been reported<sup>10</sup> and PL was observed in the region between 400 nm and 1000 nm. The exact origins of the observed PL are yet to be established, with some reports suggesting that surface effects have a significant influence<sup>11</sup>.

Germanium is a close structural and electronic analogue to Si and there has been significant interest in understanding the optical properties of Ge QDs. The vast majority of early experimental studies looked at embedded Ge QDs due to limited success in preparing free-standing samples with a controlled surface termination. It has been established<sup>12,13</sup> that in most cases the PL observed in embedded Ge QDs can be attributed to oxide related species which are mostly linked to preparation techniques (e. g. implantation into an oxide, reduction from Ge oxides, etc.). Recently, a comprehensive x-ray absorption spectroscopy (XAS) study of the nano-size effect on the structural properties of Ge QDs embedded in a silica matrix has been conducted<sup>14,15</sup> which suggests a structurally disordered region (due to static variation of bond angles and bond lengths) is formed between the nano-crystalline core and silica matrix. Again, the role of the matrix in the formation of these regions and the effect of the matrix on the optical properties of embedded Ge quantum dots is unclear. At the same time, empirical and first-principles molecular dynamics simulations<sup>16</sup> indicate the significance of surface-related structural disorder in small (1–3 nm), free standing nanoparticles. The role of this surface-induced disorder on the electronic and optical properties of small Ge QDs is yet to be explored experimentally, however it is clear that its



nature may be different from the well-known and well-studied bulk amorphous systems. The main feature of the disordered interfacial region between the core and the surface that sets it apart from the bulk amorphous counterparts is that it is structurally related to the crystalline core, which may still be present in small nanoparticles<sup>16</sup>.

Recent advances in colloidal synthesis<sup>10</sup> provided access to free-standing Ge QDs. However, the main challenge in establishing a direct link between the atomic structure and optical emission still remains. Our own early work<sup>17</sup> using a top-down approach resulted in samples that do not show significant evidence of Ge-based oxides as characterised by Raman spectroscopy<sup>18</sup> and EDX analysis, while FTIR/Raman data show the presence of Ge hydroxide/hydride species. These synthesis methods provide access to matrix-free Ge QDs with hydrogen and oxygen terminated surfaces providing very promising model systems for studying the complex nature of size and surface effects.

One technique that is capable of linking light emission directly with the structure is optically-detected XAS (OD-XAS). OD-XAS is a technique that enables structural data to be obtained directly from x-ray excited optical luminescence (XEOL) and has already been used to address the origins of PL in *p*Si<sup>6,19,20</sup>. OD-XAS is based on sensitivity of the XEOL signal to photoelectron generation in the x-ray absorption process near and above the x-ray absorption edge of an element (see Fig. 1). The XEOL-related x-ray absorption signal is measured by recording the integral photoluminescence yield within a selected wavelength range. Thus, OD-XAS is sensitive to a subset of sites related to the light emission. Despite its capabilities, OD-XAS could not provide an unambiguous answer as to the origins of PL in *p*Si. One of the main reasons for that is the sensitivity of OD-XAS to the sample preparation methods<sup>21,22</sup> which precluded wider use of the technique. Another difficulty is in assessing the spatial sensitivity of this method on the scale of a few nm<sup>19,20</sup>.

Here, our objective was to understand whether optical photons produced as a consequence of an X-ray absorption process can be linked with a specific atomic structure in matrix-free Ge QDs. We demonstrate that by combining careful sample preparation, OD-XAS, and molecular dynamics (MD) simulations it is possible to extract local structure information for the light emitting site and to obtain the details of the structural morphology of a nanoparticle. In order to do that we turn our attention to the structural origin of visible PL observed in a series of Ge QDs: (i) hydrogen-terminated surface; (ii) oxygen-terminated surface; (iii) embedded into SiO<sub>2</sub> matrix.

## Results

The free-standing Ge QDs were prepared by etching<sup>17,18</sup> and the silica-embedded Ge quantum dots were prepared by sol-gel syn-

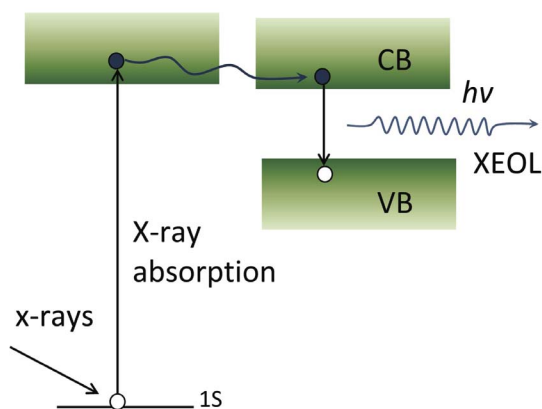


**Figure 1** | A schematic diagram of the x-ray excitation-photoluminescence cycle in OD-XAS. An excitation from a  $1s$  state to continuum followed by radiative recombination (XEOL) that carries information about a XAS event.

thesis<sup>23</sup>. The surface of some of the samples prepared by etching was oxidized by exposure to air for two weeks prior to x-ray absorption experiments. No further treatment has been done to the SiO<sub>2</sub> encapsulated samples prepared by sol-gel synthesis. Presence of Ge nanoparticles was verified by the Raman measurements and all samples showed a broad peak just below 300 cm<sup>-1</sup> corresponding to the TO-like phonon mode of the diamond-type structure (see Supplement). The size of the Ge QDs was evaluated from TEM and from Raman measurements (using the relationship described previously<sup>24</sup>) and was found to be between 5 nm and 9 nm.

A comparison of the results of the analysis of the transmission and OD-XAS data collected at the Ge K-edge at  $T = 100$  K for all three types of QDs studied are shown in Fig. 2. XEOL signal used to acquire the OD-XAS data can be seen in Fig. 2, a. The OD-XAS data obtained from XEOL are shown in Fig. 2, b. These data were used to extract the corresponding extended x-ray absorption fine structure (EXAFS) signals from which detailed structural information was obtained (see Supplement). Looking at the positions of the peaks in the magnitude of the Fourier Transform (FT) of EXAFS for oxygen-terminated samples collected in transmission mode (Fig. 2, c) one can see the signal corresponding to Ge-O bond at around 1.7 Å together with the signal at 2.45 Å corresponding to Ge-Ge bond in a diamond-type structure (see Table I in the Supplement for details). The relatively strong Ge-O peak (see Fig. 2, c) indicates significant oxygen content in oxidised samples. In OD-XAS data for oxygen-terminated samples no coordination shell at around 2.45 Å is observed at all while Ge-O signal can still be clearly seen (Fig. 2, d). For the hydrogen-terminated sample we find that only signals corresponding to Ge coordination shells are observed in transmission data and no oxygen related peaks are detected while hydrogen atoms are too weakly scattering to be seen. In the data extracted from OD-XAS of the hydrogen terminated sample once again only Ge-Ge signal is detected. However, this time only a single peak was observed corresponding to the first coordination shell. These results suggest that OD-XAS provides information different from that obtained from the transmission data as it is sampling substructures contributing to the luminescence.

In the FT extracted from OD-XAS data (Fig. 2, d) one can clearly observe the difference in the position of the first peak (corresponding to the nearest neighbours) for oxygen and hydrogen-terminated samples. In oxygen-terminated samples the first peak is located at around 1.7 Å and corresponds to the oxygen environment (Ge-O bond, see details in Table II of the Supplement). We can conclude that in oxygen-terminated samples it is the oxygen-rich content that gives the major contribution to the OD-XAS (and hence to the light emission) as we see virtually no signal from the coordination shell corresponding to the Ge-Ge distance (a coordination shell at around 2.45 Å). From this point on we only performed detailed analysis of the hydrogen-terminated sample as the data clearly indicated that OD-XAS is associated with a pure Ge phase rather than oxide. The EXAFS analysis for the hydrogen-terminated sample revealed a single peak at  $R = 2.44 \pm 0.01$  Å from the central atom which is consistent with the corresponding value for the diamond-type structure of *c*-Ge. However, we did not observe a multi-shell structure in the magnitude of the FT which is common for *c*-Ge at these temperatures<sup>25</sup>. The lack of the structural signal beyond the first shell is usually an indication of a topologically disordered (e.g. amorphous) structure. In small nanoparticles this can be due to the disorder at the interface between the surface and the core<sup>14-16,26</sup>. However, the signal may also be due to the hydrogen-terminated surface where local coordination numbers can be low. In principle, an accurate value of the coordination number can help to differentiate between the two options. A reduced coordination number in the first shell as compared to the bulk sample can be an indication that the structure is at the surface, but extracting coordination numbers from OD-XAS with a sufficiently small error margin can be a challenge due to the

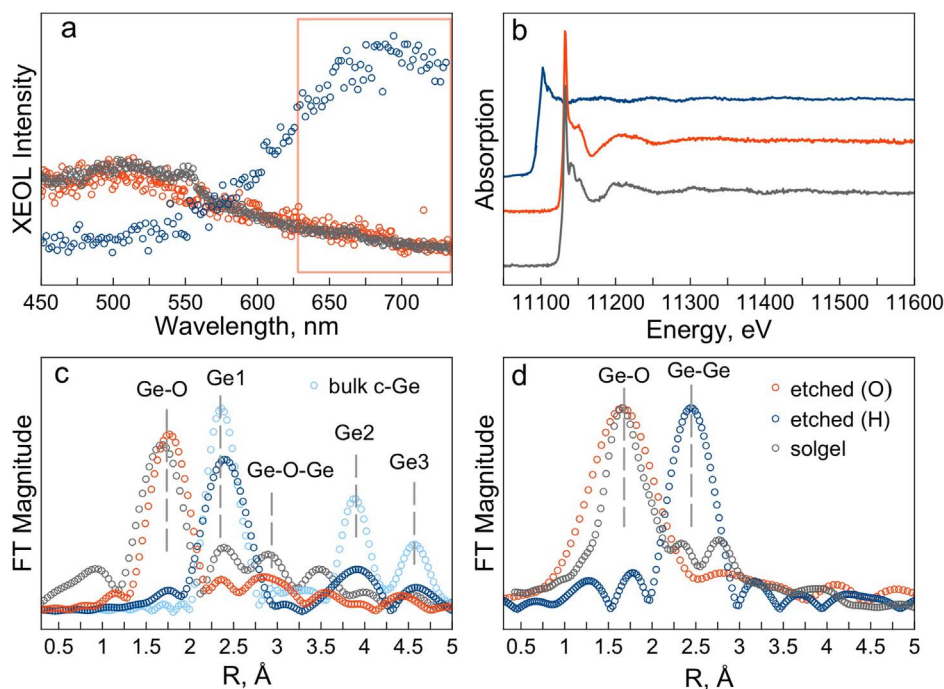


**Figure 2** | XEOL, the corresponding OD-XAS, and structural data for Ge QDs. (a), XEOL data used to extract structural information. Red rectangle indicates the position of the band used to collect OD-XAS. (b), OD-XAS data used to obtain structural information. Data for oxygen-terminated samples are shifted along x-axis for clarity. (c), Structural data extracted from transmission measurements and presented as the normalized magnitude of the Fourier transform. Reference bulk c-Ge data are also shown and positions of the coordination shells related to the oxide and pure Ge are marked (Ge1, Ge2 and Ge3 corresponds to first, second and third shells in diamond-type Ge). (d), Structural data extracted from OD-EXAFS presented as the normalized magnitude of the Fourier transform (see Methods section) with the coordination shells around Ge marked, and sample surface conditions indicated in parentheses.

complex nature of the electron excitation-de-excitation processes<sup>19,21,22,27</sup> that can affect the signal amplitude. Furthermore, the number of relevant structural parameters (e.g. atomic distances, numbers of neighbours, Debye-Waller factors) that can be reliably extracted from the data is limited by the well-known Nyquist theorem<sup>28</sup>. These parameters can be highly correlated leading to increased errors. This makes it virtually impossible to ascertain whether the OD-XAS signal originates from the whole of the nanoparticle, from only its surface, or from the disordered interface based solely on the analysis of coordination numbers.

One way to overcome the problem of parameter correlation and of their number is to use an additional source of information to fix (or constrain) as many parameters as possible in order to reduce correlations and their associated errors. A detailed model of a Ge QD could be very helpful to improve the precision of the structural information extracted from OD-XAS by placing constraints on the refined parameters. In the following analysis we used an MD-generated model of a single QD of an appropriate size (5 nm) to establish if we can further localise the source of the light emission.

To understand the effect of reduced dimensionality on the OD-XAS signal and to provide a source of information to constrain structural parameters (e.g. distances and numbers of neighbours), we have performed MD simulations of bulk Ge (to test simulation settings) and of a Ge QD. The system size was approximately 50 Å involving about 6,000 atoms. The bulk configuration with periodic boundary conditions was equilibrated for 50 ps at 100 K. To simulate a finite-size Ge nanoparticle with a free surface the cell size was increased by 20 Å - a distance larger than the potential cut-off. This resulted in atoms in the outmost layers being connected to vacuum, and induced surface relaxation (see Fig. 3, a). To quantify the effect of surface relaxation we have extracted the radial distribution functions (RDF) as a function of distance  $d$  from the surface towards the centre of the particle. In Fig. 3, b we plot RDFs for different values of  $d$ , and

observe a clear bi-modal distribution of distances at the interface between the core and the surface as  $d$  increases towards the centre of a nanoparticle. This bi-modal distribution suggests that the interfacial layer is structurally different from the crystalline core. This in turn would suggest a distinctive difference in the electronic and optical properties of the interface as compared to that of the core.

## Discussion

It is not possible to observe the level of structural detail obtained from MD in OD-XAS since MD data give positions of nuclei while EXAFS is sensitive to the electron density distribution. As a consequence, the same level of detail cannot be recovered in the magnitude of the FT for direct comparison to the MD data. However, if the XEOL emission is associated with surface states only, a shortening of the average interatomic distance down to  $\approx 2.42$  Å should be observed in the data extracted from OD-XAS (see Fig. 3, b). We observe no obvious shortening of the interatomic distance in our OD-XAS experimental data and hence conclude that the OD-XAS signal does not originate from the surface. However, the cumulant analysis of the first neighbour Ge-Ge peak ( $R = 2.44 \pm 0.01$  Å) in the OD-XAS data indicates a non-zero value of the third cumulant ( $0.005 \pm 0.003$  Å<sup>3</sup>, skewness of the peak) while third cumulants in the bulk crystalline reference sample and in the transmission signal are close to zero ( $0.0003 \pm 0.0018$  Å<sup>3</sup> and  $0.0009 \pm 0.0021$  Å<sup>3</sup> respectively). At the temperature of our experiment ( $T = 100$  K) this peak skewness suggests that there is a static contribution to the Ge-Ge peak associated with structures with distinctly different interatomic distances. This is not inconsistent with the bi-modal distribution of distances we observe in the RDFs obtained from the MD simulation (Fig. 3, b). Therefore, we used information from RDFs to constrain the refinement of OD-XAS data in order to investigate the origins of peak skewness and to recover the sub-structure responsible for the

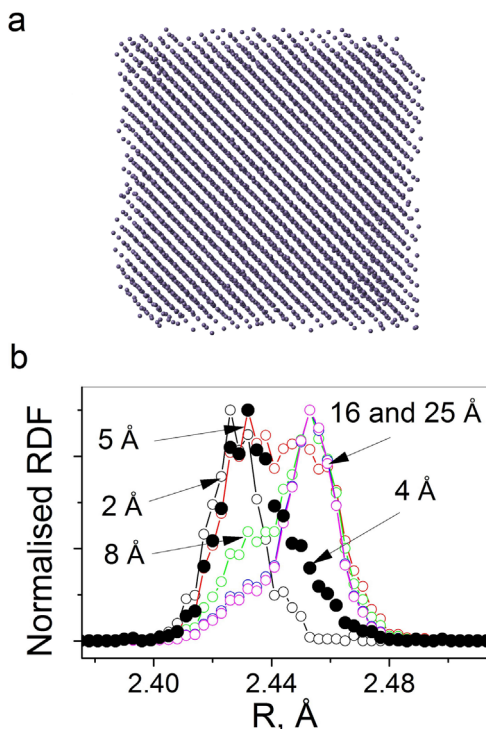


**Figure 3 | Results obtained from molecular dynamics simulations.** (a), a 5 nm Ge particle generated by molecular dynamics simulations with the surface showing clear signs of disorder. (b), RDFs extracted as a function of distance  $d$  from the surface. Numbers in Å designate a corresponding RDF.

observed OD-XAS signal. Specifically, the average number of neighbours associated with the first (surface-core interface) peak, the second (core) peak and the ratio of the corresponding peaks were used as set parameters. This information was then used to generate an EXAFS signal and to compare the model with the experiment for a number of RDFs between 2 Å and 25 Å. This allowed us to reduce the number of variable parameters to just two during a refinement: a single nearest neighbour number and a single Debye-Waller factor. The result of this comparison can be seen in Fig. 4. We found a clear minimum in the value of the fit index (which characterizes the “goodness” of a fit) for the RDF corresponding to the 5 Å layer. This result suggests that the origin of the light emission can be localized to a layer extending to around 5 Å from the surface towards the centre of the particle generated by MD.

The result above seems to suggest that it’s possible to localise the source of the light emission with sub-nanoparticle precision. At this point it is important to verify if an optical photon contributing to the extracted OD-EXAFS signal following an x-ray absorption process is produced within the specific luminescent sub-region of the sample or, as in the present case, a single nanoparticle. To address this question it is instructive to look into the nature of the OD-XAS process in relation to the nanostructures in order to understand under what conditions such a level of spatial localisation can be expected. Theoretical approaches to describe XEOL yield (and therefore localisation of OD-EXAFS) have been developed previously for bulk samples<sup>21,22</sup>. These can be adapted and applied to nanoparticles where we would expect to obtain (in the limit of small sample thickness) for variation of XEOL in a system consisting of a core, a surface and of an interface layer:

$$I_{XEOL}^{EXAFS}(E, \lambda) \propto \sum_{i,j=1}^3 \eta_j(\lambda) \chi_i(E), \quad (1)$$

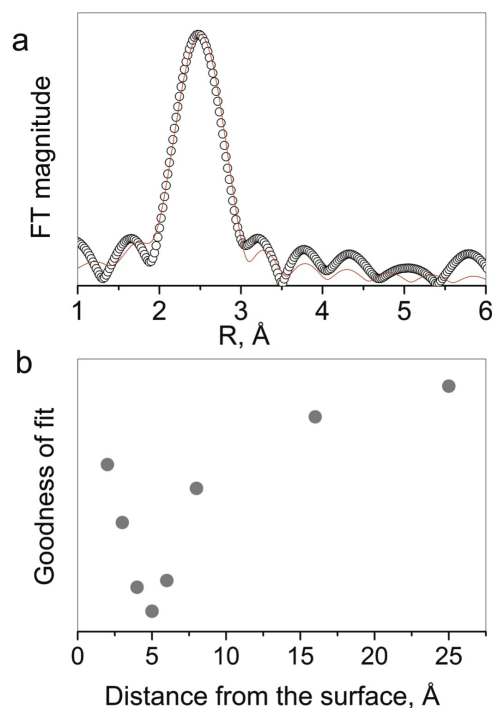


**Figure 4 | Results of the fitting of molecular dynamics based models to OD-XAS derived data.** (a), Experimental data and the best fit. (b), Goodness of fit for various RDFs calculated as a function of distance from the surface towards the center of the QD.

where  $\eta$  is the term describing photoluminescence yield (including spatial information about the decay of x-ray excited electrons to an energy level leading to the light emission),  $\lambda$  is the XEOL light emission wavelength,  $\chi_i$  is the normalised EXAFS signal, and  $E$  is the x-ray photon energy. In this notation the case of  $i = j$  corresponds to the process of x-ray absorption leading to the light emission (XEOL) within the same structural region, while  $i \neq j$  corresponds to the absorption and the emission sites being spatially separated (e.g. absorption events in the core result in light emission from the surface). This suggests that both the EXAFS process and the corresponding electron de-excitation events with the subsequent light emission must be localised to the same region of interest.

The presence of cross-terms depends on the level of localisation of  $\chi$  (the EXAFS signal) and of  $\eta$  (the light yield due to electron de-excitation down to the bottom of the conduction band). Localisation of the EXAFS signal is well understood and is related to the electron mean-free path (EMFP) of the x-ray excited core electrons. For bulk crystalline Ge it has been shown<sup>29</sup> that the EMFP is between 3 Å and 10 Å for electron energies in the EXAFS region (50–1000 eV). In structurally disordered systems this value can be even smaller<sup>30</sup> thus placing the lower limit on the accuracy of the structural localisation. This lower limit is not inconsistent with our findings.

The light yield term,  $\eta$ , originates from the de-excitation of high energy electrons to the energy levels that result in the light emission (e.g. the bottom of the conduction band, see Fig. 1). The exact nature of the de-excitation process is rather complex<sup>31</sup> and it is nearly impossible to put a single number on the value of the associated mean-free path. Nevertheless, the value of the EMFP for low energy electrons produced by de-excitation to the bottom of the conduction band can be relatively large (i.e. significantly more than 10 Å<sup>22,29</sup>) leading to the cross-terms in the Eq. 1 above. Still, if either (or both)  $\eta$  or  $\chi$  in the cross-terms should turn out to be small (compared to  $i = j$  terms) because of the low efficiency of the corresponding emission channel or low absorption by (e.g. low mass fraction of) the specific region, then OD-XAS can provide a good level of localisation. We



believe, that the level of localisation reported here is due to a combination of relative fractions of the corresponding structural components (e.g. of GeO<sub>2</sub> and/or of disordered Ge) and of the relatively high efficiency of the associated emission channels.

The level of structural localisation we report here is based on a specific morphological model - that of a layered QD with a surface, a crystalline core and a disordered interface. However, the result has general validity beyond this model in that in hydrogen-terminated Ge nanoparticles it is the disordered structural component at the interface between the core and the surface that contributes to the light emission. Another important point is that MD simulations allow one to obtain a detailed structural model that can be used as a guide to constrain (or reduce the number of) parameters used in EXAFS refinement thus improving the precision with which structural parameters are extracted. This model, if consistent with the experimental data, can further be used to examine the structural and optical properties of a system.

In summary, we demonstrate that a combination of MD simulations and OD-XAS can be used to obtain structural information about regions contributing to the light emission in Ge QDs, thus potentially providing sub-nanoparticle resolution. We show that in Ge QDs the contribution to photoluminescence crucially depends on the surface termination. In samples with an oxidised surface there is a clear contribution from the oxide to the light emission. In hydrogen-terminated samples, with the aid of molecular dynamics simulations, we show that the luminescent part of the sample probed by OD-XAFS has a disordered structure, similar to that found in the several Å thick surface layer of the nanoparticle simulated by MD. We find that light emission in Ge QDs can be directly linked to the structure and to sample preparation conditions, thus providing a direct link between synthesis and optical properties of nanostructures.

## Methods

OD-XAS experiments using the x-ray excited optical luminescence (XEOL) signal have been conducted at beamline B18 at Diamond Light Source. All data were collected at the Ge K-edge ( $\approx 11$  keV) with samples prepared so as to utilise the advantages of the thin limit<sup>21</sup> to ensure consistency between transmission and optically-detected signals. The detection system consisted of a Triax 190 spectrometer equipped with a Synapse CCD and a Newport VIS Femtowatt photoreceiver. A Hamamatsu R3809U-50 MCP photomultiplier was used for low signal conditions. The light was delivered to the spectrometer using an optical fibre. All experiments have been conducted at  $T = 100$  K using a cryojet system. OD-XAS data were reduced with PySpline<sup>32</sup> and analysed using EXCURVE<sup>33</sup> and FEFF<sup>34</sup> codes. The value of “goodness of fit”<sup>35</sup> was used to identify the best fit of the structural models generated by MD to the experimental data by varying the relevant structural parameters (e.g. interatomic distance and Debye-Waller factor). Transmission EXAFS data were used for reference.

For the MD simulations we used DL POLY MD package<sup>36</sup>, and employed the highly successful and widely used environment-dependent Tersoff potential<sup>37</sup>, particularly well suited for surface simulations where the atomic environment is different from that in the bulk.

- Alivisatos, A. P., Harris, A. L., Levinos, A. J., Steigerwald, M. L. & Brus, L. E. Electronic states of semiconductor clusters - homogeneous and inhomogeneous broadening of the optical-spectrum. *J. Chem. Phys.* **89**, 4001–4011 (1988).
- Brus, L. E. A simple model for the ionization potential, electron affinity, and aqueous redox potentials of small semiconductor crystallites. *J. Chem. Phys.* **79**, 5566–5571 (1983).
- Canham, L. T. Silicon quantum wire array fabrication by electrochemical and chemical dissolution of wafers. *Appl. Phys. Lett.* **57**, 1046–1048 (1990).
- Prokes, S. M. Light emission in thermally oxidized porous silicon: Evidence for oxide-related luminescence. *Appl. Phys. Lett.* **62**, 3244–3246 (1993).
- Brandt, M. S., Fuchs, H. D., Stutzmann, M., Weber, J. & Cardona, M. The origin of visible luminescence from porous silicon: A new interpretation. *Solid State Commun.* **81**, 307–312 (1992).
- Daldosso, N. *et al.* Role of the interface region on the optoelectronic properties of silicon nanocrystals embedded in SiO<sub>2</sub>. *Phys. Rev. B* **68**, 085327 (2003).
- Sychugov, I., Juhasz, R., Valenta, J. & Linnros, J. Narrow luminescence linewidth of a silicon quantum dot. *Phys. Rev. Lett.* **94**, 087405 (2005).
- Godefroo, S. *et al.* Classification and control of the origin of photoluminescence from Si nanocrystals. *Nature Nanotechnology* **3**, 174–178 (2008).
- Hannah, D. C. *et al.* On the origin of photoluminescence in silicon nanocrystals: Pressure-dependent structural and optical studies. *Nano Letters* **12**, 4200–4205 (2012).
- Vaughn, D. D. & Schaak, R. E. Synthesis, properties and applications of colloidal germanium and germanium-based nanomaterials. *Chem. Soc. Rev.* **42**, 2861–2879 (2013).
- Hinds, S. *et al.* Nir-emitting colloidal quantum dots having 26% luminescence quantum yield in buffer solution. *J. Am. Chem. Soc.* **129**, 7218–7219 (2007).
- Zacharias, M. & Fauchet, P. M. Blue luminescence in films containing Ge and GeO<sub>2</sub> nanocrystals: The role of defects. *Appl. Phys. Lett.* **71**, 380–382 (1997).
- Kartopu, G. *et al.* Can chemically etched germanium or germanium nanocrystals emit visible photoluminescence? *Phys. Status Solidi A* **202**, 1472–1476 (2005).
- Araujo, L. L., Kluth, P., de, M. Azevedo, G. & Ridgway, M. C. Vibrational properties of Ge nanocrystals determined by EXAFS. *Phys. Rev. B* **74**, 184102 (2006).
- Backman, M. *et al.* Amorphization of Ge and Si nanocrystals embedded in amorphous SiO<sub>2</sub> by ion irradiation. *Phys. Rev. B* **80**, 144109 (1988).
- Pizzagalli, L., Galli, G., Klepeis, J. E. & Gygi, F. Structure and stability of germanium nanoparticles. *Phys. Rev. B* **63**, 165324 (2001).
- Kartopu, G. *et al.* On the origin of the 2.2–2.3 eV photoluminescence from chemically etched germanium. *J. Luminescence* **101**, 275–283 (2003).
- Kartopu, G., Sapelkin, A. V., Karavanskii, V. A., Serincan, U. & Turan, R. Structural and optical properties of porous nanocrystalline Ge. *J. Appl. Phys.* **103**, 113518 (2008).
- Pettifer, R. F. *et al.* X-ray excited optical luminescence (xeol) study of porous silicon. *Physica B* **208 & 209**, 484–486 (1995).
- Dalba, G., Fornasini, P., Grisenti, R., Daldosso, N. & Rocca, F. On the sensitivity of the x-ray excited optical luminescence to the local structure of the luminescent sites of porous silicon. *Appl. Phys. Lett.* **74**, 1454–1456 (1999).
- Emura, S. *et al.* Optical-luminescence yield spectra produced by x-ray excitation. *Phys. Rev. B* **47**, 6918–6930 (1993).
- Goulon, J., Tola, P., Lemonnier, M. & Dexper-Ghys, J. On a site-selective EXAFS experiment using optical emission. *Chem. Phys.* **78**, 347–356 (1983).
- Henderson, E. J., Seino, M., Puzzo, D. P. & Ozin, G. A. Colloidally stable germanium nanocrystals for photonic applications. *ACS Nano* **4**, 7683–7691 (2010).
- Campbell, I. H. & Fauchet, P. M. The effects of microcrystal size and shape on the one phonon Raman spectra of crystalline semiconductors. *Solid State Commun.* **58**, 739–741 (1986).
- Sapelkin, A. V. & Bayliss, S. C. Distance dependence of mean-square relative displacements in EXAFS. *Phys. Rev. B* **65**, 172104 (2002).
- Williamson, A. J. *et al.* Probing the electronic density of states of germanium nanoparticles: A method for determining atomic structure. *Nano Letters* **4**, 1041–1045 (2004).
- Pettifer, R. & Bourdillon, A. Site-selective EXAFS via optical de-excitation. *J. Phys. C* **20**, 329–335 (1987).
- Stern, E. A. Number of relevant independent points in x-ray-absorption fine-structure spectra. *Phys. Rev. B* **48**, 9825–9827 (1993).
- Tanuma, S., Powell, C. J. & Penn, D. R. Calculations of electron inelastic mean free paths. *Surf. Interface Anal.* **36**, 1–14 (1997).
- Mott, N. F. & Davis, E. A. *Electronic Processes in Non-Crystalline Materials* (Oxford University Press, 2012).
- Erbil, A., Cargill, G. S., Frahm, R. & Boehme, R. F. Total-electron-yield current measurements for near-surface extended x-ray-absorption fine structure. *Phys. Rev. B* **37**, 2450–2464 (1988).
- Tenderholt, A., Hedman, B. & Hodgson, K. O. Pyspline: A modern, cross-platform program for the processing of raw averaged XAS edge and EXAFS data. *AIP Conf. Proc.* **882**, 105–107 (2006).
- Tomčić, S. *et al.* New tools for the analysis of EXAFS: The DL EXCURV package. Report DL-TR-2005-001, Council for the Central Laboratory of the Research Councils (2004).
- Rehr, J. & Albers, R. Theoretical approaches to x-ray absorption fine structure. *Rev. Mod. Phys.* **72**, 621–654 (2000).
- Lytle, F. W., Sayers, D. F. & Stern, E. A. Report of the international workshop on standards and criteria in x-ray absorption spectroscopy. *Physica B* **158**, 701–722 (1989).
- Todorov, I. T., Smith, B., Dove, M. T. & Trachenko, K. DL poly 3: new dimensions in molecular dynamics simulations via massive parallelism. *J. Mater. Chem.* **16**, 1911–1918 (2006).
- Tersoff, J. Modeling solid-state chemistry: Interatomic potentials for multicomponent systems. *Phys. Rev. B* **39**, 5566–5568 (1989).

## Acknowledgments

The beamtime provision by Diamond Light Source are gratefully acknowledged. W. Little is grateful to South East Physics Network for financial support.

## Author contributions

The samples were produced by A.K. OD-XAS experiments were performed by A.V.S., A.K. and W.L. under the supervision of beamline scientists G.C., R.T., F.M. and A.J.D. G.M. contributed to experimental discussions and data analysis. MD simulations were performed



by D.B. and K.T. A.V.S. wrote the paper with contributions from W.L. on the OD-XAS model.

### Additional information

**Supplementary information** accompanies this paper at <http://www.nature.com/scientificreports>

**Competing financial interests:** The authors declare no competing financial interests.

**How to cite this article:** Little, W. *et al.* Structural origin of light emission in germanium quantum dots. *Sci. Rep.* **4**, 7372; DOI:10.1038/srep07372 (2014).



This work is licensed under a Creative Commons Attribution-NonCommercial-NoDerivs 4.0 International License. The images or other third party material in this article are included in the article's Creative Commons license, unless indicated otherwise in the credit line; if the material is not included under the Creative Commons license, users will need to obtain permission from the license holder in order to reproduce the material. To view a copy of this license, visit <http://creativecommons.org/licenses/by-nc-nd/4.0/>